

# Molecular ordering in isonicotinic acid on rutile $\text{TiO}_2(110)$ investigated with valence band photoemission

James N. O'Shea<sup>a)</sup> and Janine C. Swarbrick

*School of Physics and Astronomy, University of Nottingham, Nottingham NG7 2RD, United Kingdom*

Katharina Nilson and Carla Puglia

*Department of Physics, Uppsala University, Box 530, 751 21 Uppsala, Sweden*

Barbara Brena and Yi Luo

*Theoretical Chemistry, Royal Institute of Technology, SCFAB, SE-10691 Stockholm, Sweden*

Vin R. Dhanak

*Daresbury Laboratory, Warrington, Cheshire WA4 4AD, United Kingdom,  
and Department of Physics, University of Liverpool, Liverpool L69 7ZE, United Kingdom*

(Received 14 May 2004; accepted 9 August 2004)

The adsorption of isonicotinic acid on rutile  $\text{TiO}_2(110)$  has been investigated using synchrotron-based valence band photoemission. Structural ordering in multilayer films of the molecules is found to give rise to a strong angular dependence in the valence band intensities when measured using linearly polarized radiation. Molecular ordering in this case is proposed to be induced by intermolecular hydrogen bonding which is found to be highly dependent upon the deposition rate of the isonicotinic acid. Through comparison of the experimental data with density functional calculated valence band spectra of hydrogen-bonded isonicotinic acid molecules, we can account for the angular dependence in terms of the spatial distribution of the molecular orbitals. © 2004 American Institute of Physics. [DOI: 10.1063/1.1802292]

## I. INTRODUCTION

Pyridinecarboxylic acids are a class of molecules which exhibit extensive hydrogen bonding between the nitrogen atom and the carboxylic group.<sup>1,2</sup> This is of great interest in the area of nanoscale self-assembly where exploitation of the bonding properties of such molecules might lead to the formation of nanostructures on surfaces via noncovalent interactions.<sup>3</sup> In addition, these molecules represent the fundamental building blocks of dye molecules such as those used in dye-sensitized solar cells.<sup>4-7</sup> These structures (Grätzel cells) are based on dye molecules chemically bonded to  $\text{TiO}_2$ , and thus the study of simpler related molecules such as pyridinecarboxylic acids can be instrumental in gaining a greater understanding of the underlying physical process occurring in molecular photovoltaics.<sup>8-11</sup> Isonicotinic acid consists of a pyridine ring with a carboxylic group opposite the ring nitrogen (for a schematic of the molecule see Fig. 6 in Sec. III D). The molecule is known to form head-to-tail intermolecular hydrogen-bonds between the nitrogen atom and the carboxylic group of a neighboring molecule, which represents the bulk crystallographic structure.<sup>12</sup> Monomers of isonicotinic acid have recently been shown<sup>13,14</sup> to bond to the surface of rutile  $\text{TiO}_2(110)$  through the oxygen atoms in the deprotonated carboxylic group to titanium atoms in the surface. In this so-called 2M bidentate bonding configuration the molecule has been shown to stand upright on the surface with the ring-N atom directed into vacuum. Highly ordered structures can therefore arise in the

multilayer via the head-to-tail hydrogen-bond interactions of subsequently adsorbed molecules. It has been demonstrated previously<sup>1,2</sup> that such structures can be prepared on the surface of  $\text{TiO}_2(110)$  and investigated using x-ray absorption spectroscopy (XAS) and core-level photoemission (XPS) to characterize the effect of the formation of hydrogen-bonds on the chemical environment of the ring-nitrogen atom and on the unoccupied density of states. It was found that large chemical shifts were observed in both the N1s XPS and XAS in the presence of hydrogen-bonding, in complete agreement with density functional calculations of the hydrogen-bonded molecules.<sup>1,2</sup> Furthermore, the extent of hydrogen-bonding has been shown to be related to the deposition rate such that intermolecular hydrogen-bonding in the film can effectively be turned on and off.

The focus of this current work is to extend this investigation into the valence band region to find an indicative signature for the presence of hydrogen-bonding and to characterize the effect that such an interaction would have on the electronic structure of the molecules involved.<sup>15</sup> In this paper we show through the use of valence band photoemission using linearly polarized light, and through density functional calculations, that the perturbation to the electronic structure of the molecules is only very subtle in the presence of hydrogen bonding. However, a significant dependence upon the polarization angle of the incoming radiation arises under certain growth conditions suggesting a high degree of molecular ordering which can be turned on and off in line with previous studies of hydrogen bonding in this molecule. By comparing the experimental data to density functional theory (DFT)-calculated spectra we illustrate that this angular dependence

<sup>a)</sup>Electronic mail: james.oshea@nottingham.ac.uk

is due to the spatial distribution of the molecular orbitals and their interaction with the electric-field vector of the incoming beam. Valence band photoemission using linearly polarized radiation has previously led to great insights into the symmetry and orientation of adsorbed hydrocarbon molecules,<sup>16</sup> a technique which could in principle be used to determine the orientation of isonicotinic acid molecules in an ordered multilayer.

## II. EXPERIMENT

Experiments were carried out on beamline 4.1 at the SRS, Daresbury Laboratories, UK.<sup>17</sup> The TiO<sub>2</sub>(110) single crystal substrate was obtained from Pi-Kem, Shropshire, UK, and the isonicotinic acid (99.99% pure) from Sigma-Aldrich. *P*-type semiconduction was first induced in the TiO<sub>2</sub>(110) crystal by annealing to 700 °C in  $1 \times 10^{-6}$  Torr O<sub>2</sub>, a process which leads to the formation of bulk defects.<sup>8</sup> The surface was then cleaned by sputtering with Ar<sup>+</sup> ions for 10 min followed by annealing in  $1 \times 10^{-6}$  Torr oxygen gas (99.99% pure) for 10 min at 600 °C to minimize the defects at the surface. Isonicotinic acid was deposited using a home-built retractable thermal evaporator. A monolayer was typically deposited by resistive heating of the molecule to 100 °C and depositing for 10 min during which the sample was held at 200 °C so that no multilayer adsorption would take place.<sup>13,14</sup>

Multilayer coverage of isonicotinic acid was achieved by depositing the molecules onto a monolayer sample cooled to -100 °C and maintained at this temperature for the duration of the experiment. The deposition rate for the multilayers was controlled by varying the temperature of the evaporator from 65 °C for a "slow" evaporation to 130 °C for a "fast" evaporation. In each case multilayers were deposited until the signal from the TiO<sub>2</sub> substrate was just suppressed in the Ti 2*p* XPS spectrum as measured using a low-resolution fixed x-ray anode. The thickness of the multilayer films is therefore comparable for both slow and fast preparations.

The presented valence band photoemission spectra were measured for a photon energy of 40 eV using a Scienta SES-200 hemispherical analyzer with an acceptance angle of  $\pm 5^\circ$ . An overall resolution of 200 meV was achieved. The experimental geometry of the photoemission measurements is shown in Fig. 1. The angle between the incoming radiation and the analyzer is fixed and variation of the polarization of the light with respect to the sample surface was achieved by tilting the sample. The emission angle is therefore also varied at the same time, a fact which is considered in detail in our discussion in Sec. III. The binding energy scales on the valence band spectra were calibrated to the Fermi level of the tantalum sample holder.

## III. RESULTS AND DISCUSSION

### A. Valence band of isonicotinic acid

Figure 2 shows the valence band spectra measured at normal emission angle for clean TiO<sub>2</sub> with subsequent deposition of a monolayer, and finally a multilayer of isonicotinic acid. Also shown is an estimate of the valence band spectrum

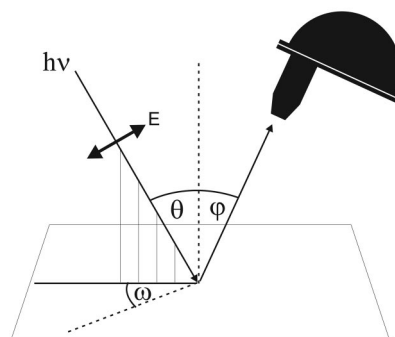


FIG. 1. Experimental geometry of the photoemission experiment.  $\theta$  is the incident radiation angle with respect to the surface normal.  $\varphi$  is the photoelectron emission angle with respect to the surface normal.  $\omega$  is the azimuthal rotation angle of the surface (fixed in this study). The sum of  $\theta$  and  $\varphi$  is also fixed by the geometry of the analysis chamber at  $54.7^\circ$ .

for an isolated monolayer of isonicotinic acid obtained by subtracting the estimated contribution of the underlying TiO<sub>2</sub> surface.

The features in the valence band spectrum of the multilayer are shifted to higher binding energy relative to the chemisorbed monolayer; this is most likely due to the reduced screening effect from the surface. The difference spectrum of the monolayer shows that the electronic structure of the molecule is not significantly modified upon chemisorption to the surface. The lower intensity of the peak at 8.5 eV (peak 2) compared with the multilayer may be due to the presence of a surface state peak in the clean TiO<sub>2</sub> spectrum used for the subtraction (which is not expected to remain in

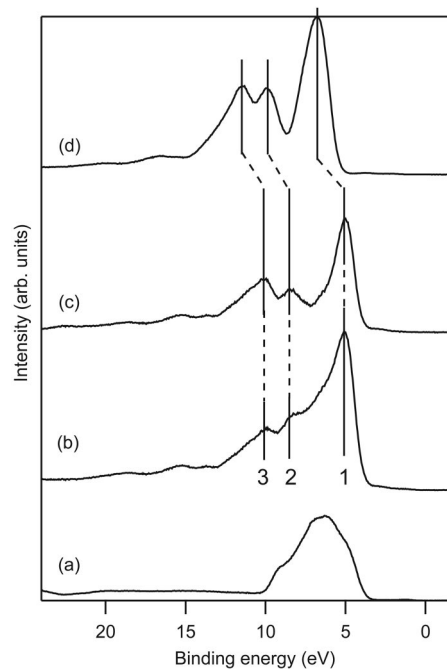


FIG. 2. Valence band spectra ( $h\nu=40$  eV) for (a) the clean TiO<sub>2</sub>(110) surface, (b) a monolayer of isonicotinic acid, (c) the monolayer spectrum with the substrate contribution subtracted ( $b-a$ ), and (d) a multilayer of isonicotinic acid. Spectra were measured at normal emission angle and normalized to the intensity of the main peak with the exception of that of the clean substrate which is shown as used in the subtraction,  $b-a$ .

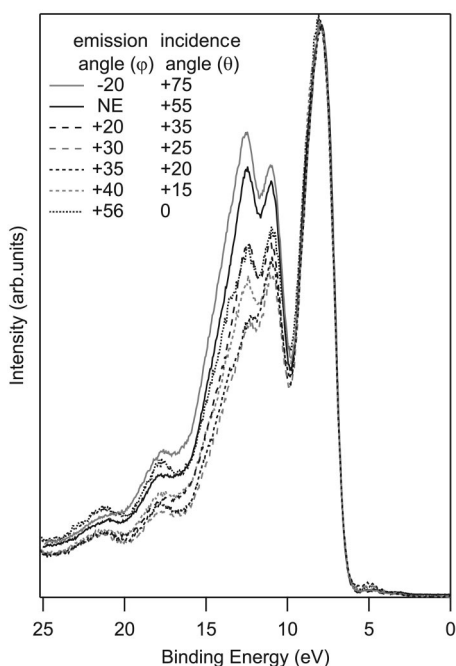


FIG. 3. Valence band spectra ( $h\nu=40$  eV) measured for a multilayer of isonicotinic acid prepared by a slow deposition of the molecule on TiO<sub>2</sub>(110) at  $-100$  °C. Spectra have been normalized to the intensity of the main peak to illustrate the dependence on the incident radiation angle  $\theta$ .

the presence of a chemisorbed monolayer). It is also worth noting that while the relative energy separations of the molecular orbital peaks 2 and 3 in the monolayer and the multilayer remain unchanged (at 1.6 eV), the relative separation of peaks 1 and 2 is increased by 0.3 eV when chemisorbed to the surface. This suggests that the highest occupied molecular orbitals are more strongly involved in the bonding of the molecules to TiO<sub>2</sub>(110) and thus enjoy a higher degree of screening from the polarizable surface.

### B. Structural ordering in isonicotinic acid multilayers

Figure 3 shows the valence band spectra ( $h\nu=40$  eV) measured over the full range of incidence and emission angles available in our experiment for a multilayer film of isonicotinic acid adsorbed on the TiO<sub>2</sub>(110) surface. In this case a slow multilayer was prepared at a sample temperature of  $-100$  °C by evaporating isonicotinic acid ( $65$  °C) onto a chemisorbed monolayer (formed at a sample temperature of  $200$  °C). The spectra have been normalized to the intensity of the first peak in the spectrum (the lowest binding energy feature) in order to illustrate the angular dependence of the data. The intensities of the peaks in the energy range from 10–25 eV relative to the intensity of the first peak show a clear angular dependence. The effect is most pronounced for the second and third lowest energy peaks at 12 and 13.5 eV, respectively. Furthermore, it is evident that it is the incidence angle and not the emission angle which plays the most important role in this dependence: if the emission angle, and consequently surface sensitivity, was the key factor, then we would expect to observe very similar spectra for  $+20$ ° and  $-20$ ° emission, in contrast to the data presented in Fig. 3. We propose therefore that the valence band spectrum is

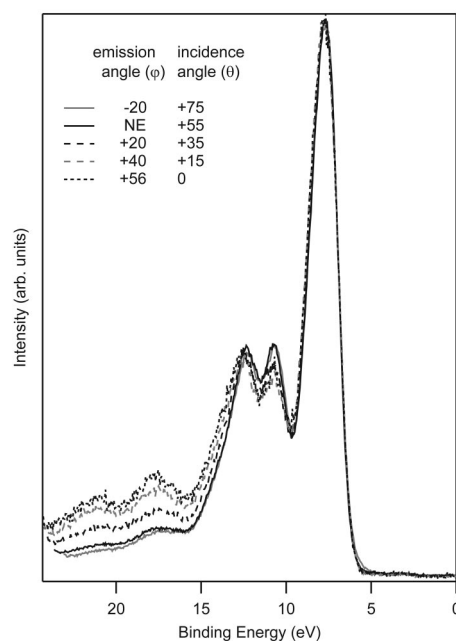


FIG. 4. Valence band spectra ( $h\nu=40$  eV) measured for a multilayer of isonicotinic acid prepared by fast deposition of the molecule on TiO<sub>2</sub>(110) at  $-100$  °C. At different incidence angles, the traces lie roughly on the same curve.

strongly dependent in this case on the angle of incidence and consequently the interaction of the electric-field vector of the incoming radiation with the molecules on the surface. It follows then that there must be a high degree of molecular ordering in the multilayer for such an effect to be observed. Molecular ordering in this case is likely to arise from the formation of intermolecular hydrogen bonds as discussed in Sec. I.

In order to further understand why the relative intensities vary with the interaction angle it is instructive to consider the assignments of the peaks in the experimental valence band. From our density functional calculations of the hydrogen-bonded molecules, which are discussed in detail in Sec. III D, we can deduce the orbital contributions to the main spectral features. The lowest binding energy peak is mainly populated by the  $2p$  orbitals of C, O, and N; these form  $\pi$  bonding C-C, C-O, and C-H orbitals and also  $\sigma$  antibonding C-C and C-H orbitals. The second lowest binding energy peak ( $\sim 12$  eV) is similarly populated, but there are large  $\pi$  bonding orbitals between all of the atoms (both C and N) in the pyridine ring. The third peak ( $\sim 13.5$  eV) contains  $\sigma$  orbitals of largely antibonding character formed by the  $2s$  atomic orbitals of all the atoms in the molecule. In the region between 15 eV and 20 eV are the C-O-H bonding orbitals, followed by C-C antibonding and C-H bonding orbitals.

The formation of intermolecular head-to-tail hydrogen bond interactions in isonicotinic acid has been observed previously via XPS and XAS to be strongly dependent upon the multilayer preparation conditions.<sup>1,2</sup> The valence band spectra shown in Fig. 4 measured for a fast deposition of isonicotinic acid further emphasize this effect on the hydrogen-bond induced structural ordering of the film. In this case a fast multilayer was prepared at a sample temperature of

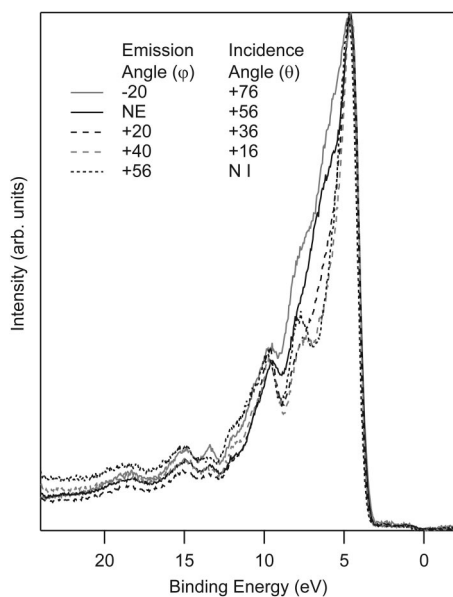


FIG. 5. Valence band spectra ( $h\nu=40$  eV) measured over a range of incidence/emission angles for a monolayer of isonicotinic acid prepared by slow deposition of the molecule on  $\text{TiO}_2(110)$  at  $200^\circ\text{C}$ . NE=normal emission, NI=Normal incidence

$-100^\circ\text{C}$  by evaporating isonicotinic acid ( $130^\circ\text{C}$ ) onto a chemisorbed monolayer (formed at a sample temperature of  $200^\circ\text{C}$ ). The spectra have again been normalized to the intensity of the main peak for direct comparison with the data shown in Fig. 3. The angular dependence is largely suppressed in this case, with the intensity ratios of the first three peaks remaining essentially unchanged with varying incidence/emission angle. This suggests a significantly more disordered film than that presented in Fig. 3, most likely due to the suppression of intermolecular hydrogen-bond formation. While the peaks above 15 eV do show some angular dependence, it is likely that this is due in this case to the increased background intensity associated with the increasingly grazing emission angles. It is also worth noting that the relative intensities of the second and third peaks with respect to the first are significantly lower in the disordered film than they are in the ordered film. In the latter case, the molecules are likely to be ordered azimuthally and therefore the azimuthal rotation angle will play a role in the way that polarized light interacts with the molecules. We therefore attribute the higher relative intensity of the second and third peaks to the preferential excitation of these orbitals at the azimuthal angle set by the experimental geometry (see Fig. 1). An experiment with variable azimuthal rotation is indeed planned to investigate this in more detail.

### C. Structural ordering in isonicotinic acid monolayers

An angular dependence is also observed for monolayers of isonicotinic acid chemisorbed to the surface of rutile  $\text{TiO}_2(110)$ , formed by depositing the molecule at a sample temperature of  $200^\circ\text{C}$ . At this temperature growth is limited to a single chemisorbed monolayer.<sup>13</sup> Figure 5 shows the valence band spectra measured for an isonicotinic acid monolayer over a range of incidence/emission angles. All of

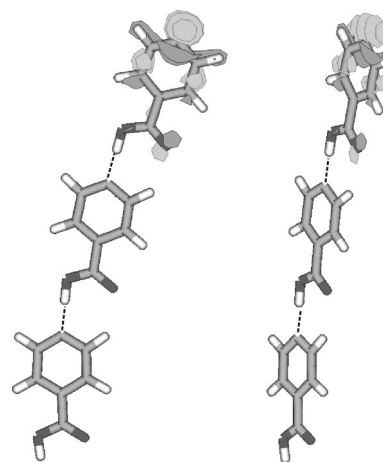


FIG. 6. Optimized geometry of the hydrogen-bonded trimer used for the density functional calculations of the valence band spectra. The spatial distribution of the highest occupied molecular orbital (HOMO) is illustrated for the top isonicotinic acid molecule. The dashed lines indicate the O-H—N intermolecular hydrogen bonds.

the spectra have again been normalized to the intensity of the first (lowest binding energy) peak and exhibit an angular dependence with respect to the incoming light. Although the spectra now contain a significant contribution from the underlying titanium dioxide substrate, the observed angular dependence is not dominated by changes in the surface sensitivity of the measurement, since the spectra obtained at  $-20^\circ$  and  $+20^\circ$  emission are very different. This suggests, as in the case of the multilayer, that there is significant molecular ordering in the monolayer and that the angular dependence is related to the interaction of the electric-field vector of the polarized light with the molecular orbitals involved. This is in agreement with a recently published model for the adsorption geometry of isonicotinic acid monolayers on  $\text{TiO}_2(110)$  in which the surface is stabilized by dimerization of the molecules through ring-ring interactions where the azimuthal orientational difference between molecules is  $60^\circ$ – $90^\circ$  and the polar angle is less than  $40^\circ$  from the surface normal.<sup>13</sup>

### D. Density functional calculations (DFT)

Density functional calculations have also been carried out in order to understand the various contributions of the molecular orbitals to the valence band spectrum and the observed angular dependence.

Molecular geometries used for calculations of the valence band spectra and molecular orbital shapes were optimized at the hybrid DFT method B3LYP with the standard 6-31G\*\* basis set using the GAUSSIAN 98 program.<sup>18</sup> The valence molecular orbital energies were determined by Koopman's theorem at the DFT/B3LYP level with a 6-31G basis set. The valence band spectral intensities are obtained according to the Gelius intensity model<sup>19</sup> and the experimental relative photoionization cross sections for the different orbitals at 40 eV excitation energy are used. The final spectra have been convoluted by a Gaussian curve of 1.0 eV full width at half maximum (FWHM). The optimized molecular geometry used for the DFT calculations is shown in Fig. 6.

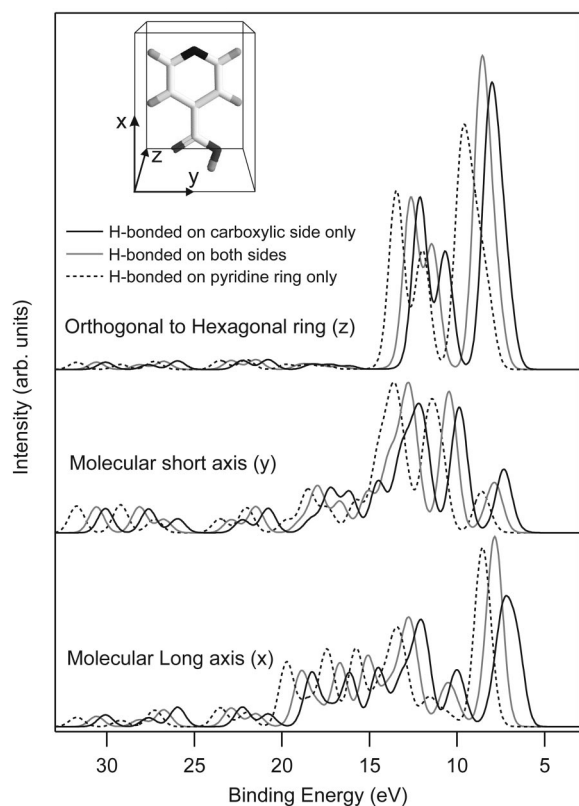


FIG. 7. DFT calculated spectra for the  $x$ ,  $y$ , and  $z$  components of the valence band. These are shown for molecules in three different chemical environments: H-bonded only on the carboxylic side; H-bonded at both sides; and H-bonded only on the pyridine ring side of the molecule

The model consists of three isonicotinic acid molecules connected by head-to-tail O—H—N intermolecular hydrogen bonds. Also shown in Fig. 6 is the spatial distribution of the highest occupied molecular orbital (HOMO) calculated for the isonicotinic acid molecule hydrogen-bonded only at the carboxylic end.

DFT calculated valence band spectra for the isonicotinic acid molecules in the three different chemical environments of our model are shown in Fig. 7. Individual spectra were calculated for the electric field vector of the linearly polarized light directed along the three orthogonal axis of the molecule,  $x$ ,  $y$ , and  $z$ . As shown in the inset of Fig. 7 the  $x$  direction is defined along the length of the molecule, the  $z$  direction is perpendicular to the pyridine ring, and the  $y$  direction is the remaining coordinate, in the plane of the molecule perpendicular to its length. It can be seen that the molecular orbitals shift to higher binding energies starting from molecules H-bonded at the carboxylic side of the molecule, through molecules having H-bond interactions at both sides, to molecules where the interaction is only through the nitrogen atom of the pyridine ring.

In terms of the relative intensities of the peaks we note that the main contribution to the highest occupied molecular orbitals comes primarily from the  $z$  plane (where the polarization is directed perpendicular to the plane of the pyridine ring) and is weakest for the molecular short axis ( $y$  plane). Conversely, the  $z$  plane contributes little intensity to any of the molecular orbitals which lie deeper than 12 eV binding

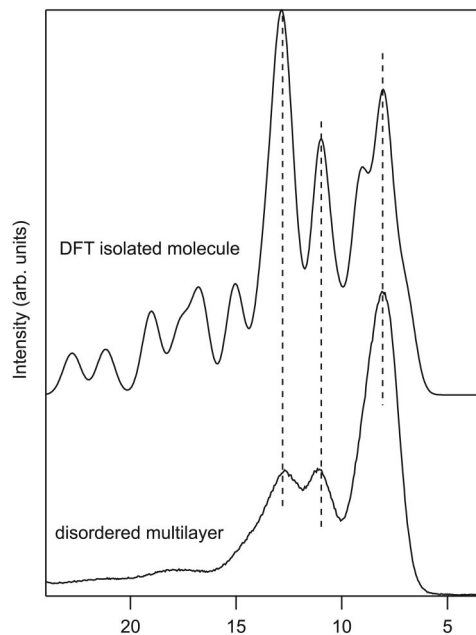


FIG. 8. Comparison of the experimental valence band spectrum ( $h\nu = 40$  eV) for a disordered multilayer film with the DFT calculated spectrum (over all three axes) for an isolated isonicotinic acid molecule.

energy, where the main contribution comes instead from the  $x$  and  $y$  planes. It is immediately apparent from these calculations that the measured valence band spectrum of isonicotinic acid will depend strongly upon the angle of interaction between the electric-field vector of the incoming radiation and the molecular plane.

In the case of a completely disordered multilayer film of isonicotinic acid the molecules may adopt every possible orientation and the measured valence band spectra should resemble an equal combination of each of the three axis-specific calculations. Furthermore, intermolecular hydrogen-bonding is not expected to play a role since such interactions would lead to structural ordering of the molecules. In order to illustrate this we present in Fig. 8 a direct comparison between the valence band spectrum calculated for an isolated isonicotinic acid molecule over all orientations and the experimental spectrum of a disordered multilayer. The agreement between the theoretical and experimental spectra is very good, with all of the key features of the valence band reproduced at the correct energies, including many of the more subtle asymmetries observed in the experimental spectrum.

In the case of a highly ordered multilayer of isonicotinic acid, where the majority of molecules are linked together in long chains via the intermolecular head-to-tail hydrogen-bonding discussed in Sec. I, the measured valence band spectrum for the multilayer will depend strongly upon the molecular orientation with respect to the incoming beam, as predicted by the DFT calculations of Fig. 7. In principle, by comparing the theoretically calculated components to valence band spectra measured over all possible orientations of the surface, the precise orientation of the molecules in an ordered multilayer could be determined. The effect of rotating the sample about precisely defined axis (with respect to

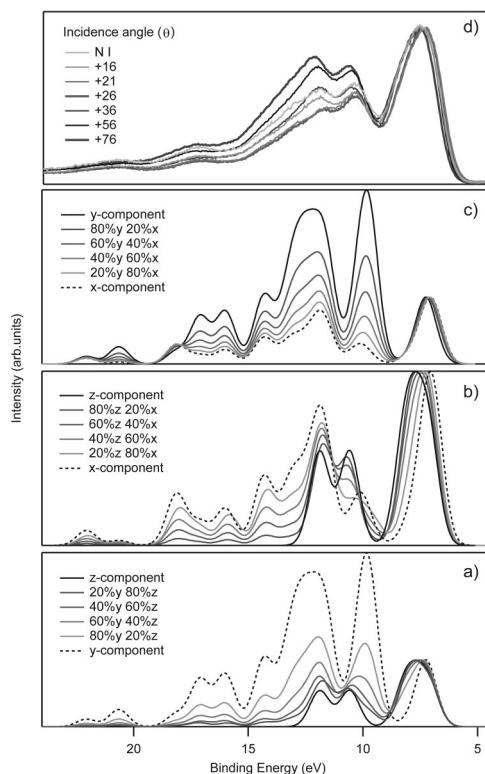


FIG. 9. DFT spectra calculated for an isonicotinic acid molecule hydrogen bonded at both ends, simulating the effect of rotating the molecule about (a) the  $x$  axis, (b) the  $y$  axis, and (c) the  $z$  axis in a beam of polarized radiation ( $h\nu=40$  eV). For comparison, the measured experimental data for an ordered multilayer of isonicotinic acid is shown in (d).

the molecular plane) is simulated in Figs. 9(a)–9(c). Here we present the various combinations of the axis-specific spectra associated with rotating the molecule with respect to the  $E$ -vector of the incoming radiation, e.g., Fig. 9(c) predicts how the valence band would change in rotating the  $E$ -vector about the  $z$  axis from being directed precisely along the short axis of the molecule ( $y$ ) to being directed along the long axis of the molecule ( $x$ ). Since the vast majority of the molecules in a highly ordered film will be H-bonded on both sides, we have used the central molecules of our model (Fig. 6) for this simulation.

In the present study, the experimental geometry provided rotation only about a single axis of the sample, fixed at an arbitrary angle in the second axis of rotation required for a complete determination of the molecular orientation. Clearly the angular dependence measured in this case [shown in Fig. 9(d)] will not therefore represent a simple rotation about a single molecular axis but rather a complex combination of the extreme cases presented in Figs. 9(a)–9(c). For this reason, we have not attempted to deduce the orientation of the molecules at the current time. However, Fig. 9 demonstrates that the origin of the angular dependence observed in the valence band does indeed arise from the changing interaction of the electric-field vector with the molecules as we rotate the ordered multilayer sample.

#### IV. CONCLUSIONS

Isonicotinic acid may be deposited onto  $\text{TiO}_2$  to form ordered multilayer structures mediated by the formation of

intermolecular head-to-tail hydrogen bonds. Depending on the growth conditions, both ordered and disordered multilayers may be grown. Slow growth conditions which promote the formation of an ordered multilayer were prepared at temperatures of  $65^\circ\text{C}$  over a period of 30 min. Fast growth conditions at  $130^\circ\text{C}$  over 2 min gave disordered multilayers, most likely due to the suppression of intermolecular hydrogen-bond formation. Valence band spectra measured over a range of incidence angles have provided a valuable insight into the molecular ordering within the multilayer and have been shown to be an effective probe for the presence of such ordering due to the spatial distributions of the corresponding molecular orbitals. The DFT calculations presented in this paper highlight the strong dependence of the valence band spectra upon the angle of interaction between the electric field vector of the incoming radiation and the molecular plane. In principle, this method could be used to determine the orientation of molecules in the film where experimental data could be measured over two axes of sample rotation. Work is currently underway to attempt this for the isonicotinic acid system.

#### ACKNOWLEDGMENTS

The authors would like to thank the Council for the Central Laboratory of the Research Councils (CCLRC) for access to the Daresbury laboratory under the direct access program, also the UK Engineering and Physical Sciences Research Council (EPSRC) and the Swedish Research Council (VR) for financial support. They are also grateful to George Miller for technical support during the beamtime.

- <sup>1</sup>J. N. O'Shea, J. Schnadt, P. A. Brühwiler *et al.*, *J. Phys. Chem. B* **105**, 1917 (2001).
- <sup>2</sup>J. N. O'Shea, Y. Luo, J. Schnadt, L. Patthey *et al.*, *Surf. Sci.* **486**, 157 (2001).
- <sup>3</sup>J. A. Theobald, N. S. Oxtoby, M. A. Phillips, N. R. Champness, and P. H. Beton, *Nature (London)* **424**, 1029 (2003).
- <sup>4</sup>M. Grätzel, *Nature (London)* **414**, 338 (2001).
- <sup>5</sup>A. Hagfeldt and M. Grätzel, *Chem. Rev. (Washington, D.C.)* **95**, 49 (1995).
- <sup>6</sup>A. Hagfeldt and M. Grätzel, *Acc. Chem. Res.* **33**, 269 (2000).
- <sup>7</sup>K. Westermark, H. Rensmo, A. C. Lees, J. G. Vos, and H. Siegbahn, *J. Phys. Chem. B* **106**, 10108 (2002).
- <sup>8</sup>P. Persson, S. Lunell, P. A. Brühwiler *et al.*, *J. Chem. Phys.* **112**, 3945 (2000).
- <sup>9</sup>J. Schnadt, J. N. O'Shea, L. Patthey *et al.*, *J. Chem. Phys.* **119**, 12462 (2003).
- <sup>10</sup>J. Schnadt, J. N. O'Shea, L. Patthey, J. Krempasky, N. Mårtensson, and P. A. Brühwiler, *Phys. Rev. B* **67**, 235420 (2003).
- <sup>11</sup>J. Schnadt, P. A. Brühwiler, L. Patthey *et al.*, *Nature (London)* **418**, 620 (2002).
- <sup>12</sup>F. Takusagawa and A. Shimada, *Acta Crystallogr., Sect. B: Struct. Crystallogr. Cryst. Chem.* **32**, 1925 (1976).
- <sup>13</sup>J. Schnadt, J. Schiessling, J. N. O'Shea *et al.*, *Surf. Sci.* **540**, 39 (2003).
- <sup>14</sup>J. Schnadt, J. N. O'Shea, L. Patthey, J. Schiessling, J. Krempasky, M. Shi, N. Mårtensson, and P. A. Brühwiler, *Surf. Sci.* **544**, 74 (2003).
- <sup>15</sup>S. A. Sardar, J. A. Syed, K. Tanaka, F. P. Netzer, and M. G. Ramsey, *Surf. Sci.* **519**, 218 (2002).
- <sup>16</sup>H. P. Steinruck, *J. Phys.: Condens. Matter* **8**, 6465 (1996).
- <sup>17</sup>V. R. Dhanak, A. W. Robinson, G. Vanderlaan, and G. Thornton, *Rev. Sci. Instrum.* **63**, 1342 (1992).
- <sup>18</sup>M. Frisch, G. Trucks, H. Schlegel *et al.*, GAUSSIAN 98 (Gaussian Inc., Pittsburgh, PA, 1998).
- <sup>19</sup>U. Gelius, *J. Electron Spectrosc. Relat. Phenom.* **5**, 985 (1974).